

Microelectrical Mechanical Systems Switch for Designing Multi-Band Antenna

A.H.M. Zahirul Alam, Md. Rafiqul Islam, Sheroz Khan, Muhammad Mahbubur Rashid
Department of Electrical and Computer Engineering, Faculty of Engineering,
International Islamic University Malaysia, Kuala Lumpur, Malaysia

Abstract: Problem statement: In this study Microelectrical Mechanical System (MEMS) switches were proposed to design a reconfigurable/multi-band antenna to replaced PIN diode switches or semiconductor switches due to lower insertion losses, good isolation, much lower intermodulation distortion, and lower power consumption. The antenna is able to operate at very high frequencies. **Approach:** A reconfigurable antenna that is capable to operate at several frequencies was proposed by introducing two adjacent patches along with main radiating patch and two MEMS switches. Parametric analysis of the size of the wing patches was done for finding optimum size. A comparative study was done for Alumina, SiN, GaAs and Teflon as MEMS bridge materials for finding better results in terms of return loss and number of bands. The design was performed by using 3D electromagnetic simulator HFSS considering ideal MEMS switches. **Results:** It was found that SiN as MEMS bridge material makes the antenna to operate at 16.76, 23.56 and 27.7 GHz in the “OFF” states and operate at 20.9 and 21.91 GHz in the “ON” states of MEMS switches. **Conclusion/Recommendations:** MEMS cantilever beam material played an important role for providing antenna to operate at multi-band frequencies. The proposed multiband/reconfigurable antenna can be implemented with easy fabrication process steps by the Sandwich method of fabrication.

Key words: Antenna, reconfigurable, RF, MEMS

INTRODUCTION

Reconfigurable multi-band antennas are attractive for many military and commercial applications where it is required to have a single common aperture antenna that can be dynamically reconfigured to transmit (or receive) on multiple frequency bands. Such common-aperture antennas lead to considerable savings in size, weight and cost. They find applications in space-based radar, communication satellites, electronic intelligence and aircraft navigations besides many other communications and sensing applications. A number of different reconfigurable antennas, such as planar and 3-D have been developed. Some of them are developed for radar applications^[1,2] and other planar antennas are designed for wireless devices^[3,4]. Reconfigurable slot antennas are designed for UHF^[5]. Reconfigurable patch antennas are also designed to operate in both L and X bands^[6].

Radio Frequency Microelectrical Mechanical Systems (RF MEMS) is an emerging technology that promises the potential of revolutionizing RF and microwave systems implementation for the next generation of telecommunication applications. Its low-power, excellent RF performance, large tuning range

and integration capability are the key characteristics, enabling system implementation with potential improvements in size, cost and increased functionality. They are normally built on high-resistivity silicon wafers, gallium arsenide (GaAs) wafers and quartz substrates using semiconductor microfabrication technology with a typical four-to six-mask level processing^[7-11]. Typical example of MEMS based antenna are reported in^[12-15]. In this study, we proposed a multi-band reconfigurable antenna using RF MEMS switches that can be fabricated with easy process steps. The effect of material used for MEMS switches is simulated and analyzed under the conditions when both the switches are either “OFF” or “ON”.

Reconfigurable MEMS antenna design: The schematic diagram of the proposed reconfigurable antenna is shown in Fig. 1. It consists of three patches placed on a 18×10 mm² Rogers substrate of thickness 0.32 mm. The centre patch of dimension 4×3 mm² and two side patches defined as wing patches, separated by gap of 0.5 mm. The co-axial feeding point is placed at the centre patch. The length of the wing patch is chosen as $L_w = 5$ mm and the width is defined as “ W_w ”.

Corresponding Author: A.H.M. Zahirul Alam, Department of Electrical and Computer Engineering, Faculty of Engineering, International Islamic University Malaysia, Kuala Lumpur, Malaysia

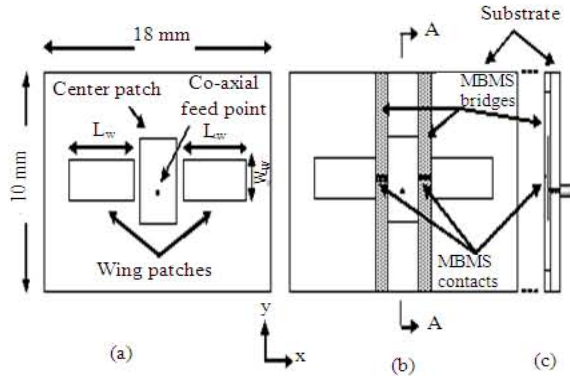


Fig. 1: Schematic diagram of MEMS reconfigurable antenna (a): Without MEMS Bridge, (b): With MEMS Bridges and (c): Cross sectional view at A-A

Cantilever type MEMS switches are considered for the design, which consist of cantilever bridges and MEMS contacts. The length of bridges is 10 long, 1 mm wide, 20 μm thick and placed above the patch gaps. The MEMS are placed on the centre of bridge with 1 mm long and 100 μm wide contacts. The distance between the patch and the MEMS is 5μm, which the MEMS are considered “OFF”.

Antenna modeling: The centre patch antenna is first designed based on the equations from the Transmission Line Model (TLM) approximation^[16], which states that the operating frequency of patch antenna is given by:

$$f_r = \frac{1}{2(L + \Delta L)\sqrt{\epsilon_{eff}}\sqrt{\mu_0\epsilon_0}} \quad (1)$$

Where:

- L = The length of the antenna
- ϵ_0 and μ_0 = The free space dielectric permittivity and permeability respectively
- ϵ_{eff} = The effective dielectric permittivity given as:

$$\epsilon_{eff} = \frac{\epsilon_r + 1}{2} + \frac{\epsilon_r - 1}{2} \left[1 + 12 \frac{h}{W} \right]^{-1/2} \quad (2)$$

Where:

- ϵ_r and h = The relative dielectric permittivity and thickness of the substrate
- W = The width of the patch

Because of the fringing effects, the antenna looks larger than its physical dimensions. The parameter ΔL

in Eq. 1 takes this effect into account and can be computed by:

$$\Delta L = 0.412h \frac{(\epsilon_{eff} + 0.3)\left(\frac{W}{h} + 0.264\right)}{(\epsilon_{eff} - 0.258)\left(\frac{W}{h} + 0.8\right)} \quad (3)$$

In order to facilitate its characterization, the antenna is designed to have matching input impedance (50 Ω) as mentioned earlier. The input impedance of the antenna can be adapted by choosing the right position for the feeding point. The impedance is maximum at the patch border and decreases as it moves in from the border, given by:

$$Z_m = Z_{max} \cos^2 \left[y \frac{\pi}{L} \right] \quad (4)$$

where, Z_{max} is the impedance at $y = 0$. Using the values given by the TLM approximation, a model for the antenna is built using HFSS. The model is used to trim the antenna dimensions for the desired frequency. The two wing patches are placed on the two sides of the centre patch to obtain reconfigurability.

MATERIALS AND METHODS

The patch antenna design is supported with a model built using a High Frequency Structure Simulator (HFSS) based on Finite Elements Modeling (FEM). A tool with 3D modeling capabilities is necessary due to the fact that, for small ground planes, the antenna behavior depends on the ground size.

The two critical steps in designing the patch antenna are the definition of the patch dimensions and the feeding configuration. The patch dimensions have direct influence on the operating frequency and on the antenna gain. The difficulty is how to predict accurately the patch dimensions, which is related to the fringing fields together with the small size of the ground plane used.

The antenna feeding should be designed carefully since it must provide a correct impedance matching. At high-signal frequencies it is necessary to design a feeding line with specific characteristic impedance. Also, that line must be connected to a point of the antenna where the input impedance is the same as that of the feed-line characteristic impedance.

A considerable amount of effort and research is done to accurately predict the electrical behavior of RF MEMS switches^[12,13]. One of the most compelling reasons for using MEMS in antenna application is that they have shown to approximate, to a very good degree,

Material	Relative permittivity (ϵ_r)	Loss tangent
GaAs	12.9	0.000
Alumina	9.4	0.006
SiN	7.0	0.000
Teflon	2.1	0.001

ideal switches. This allows us to forego the nearly impossible task (at present) of a complete field simulation of an entire antenna structure, including all the minute details of MEMS switches. Therefore, the reconfigurable antenna is designed by performed using a less complex approach with simplified equivalent switches in place of the actual MEMS structure.

The reconfigurable antenna performance depends on the separation between the centre patch and the wing patch, wings and MEMS dimensions as well as the material chosen for the MEMS cantilever bridges. Optimization has been performed by using HFSS simulator. The up and down states of both the MEMS switches are defined as “OFF” and “ON” states. The “ON” states shortened the wing and the centre patches.

The properties of the dielectric materials used for designing multiband antenna are shown in Table 1.

RESULTS

Effects of MEMS contact width: The effects of MEMS contact of width on the return loss is shown in Fig. 2, considering Alumina as a bridge material. The Fig. 2 shows that the antenna performance reduces with the increase in width of the MEMS switches whether the MEMS are in “OFF” or “ON” states. A width of 0.2 mm is chosen as the optimum width of MEMS switches considering them in “OFF” and “ON” states. It is also observed that the wide width of the MEMS switches has no effect on variation of the resonance frequency whether the MEMS are either in “OFF” or “ON” states. This indicates that the wide MEMS switches provide continuous path between centre and wing patches.

The antenna resonance frequency and the return loss with different MEMS contact width are shown in Fig. 3 when the MEMS switches are “OFF” and “ON” states. There are three resonant frequencies for the MEMS with width of 0.2 mm and less two resonant frequencies for width larger than 0.2 mm when the MEMS contacts are in the “OFF” states. It is also observed that the return loss of the antenna is higher for MEMS width larger than 0.2 mm, except for the width of 0.4 mm when the MEMS contacts are in the “OFF” states. When the MEMS contacts are in the “ON” states, there is only single resonant frequency except widths of 0.1 and 0.9 mm. However, low return loss can be obtained when the MEMS contact width is less than 0.4 mm. Therefore,

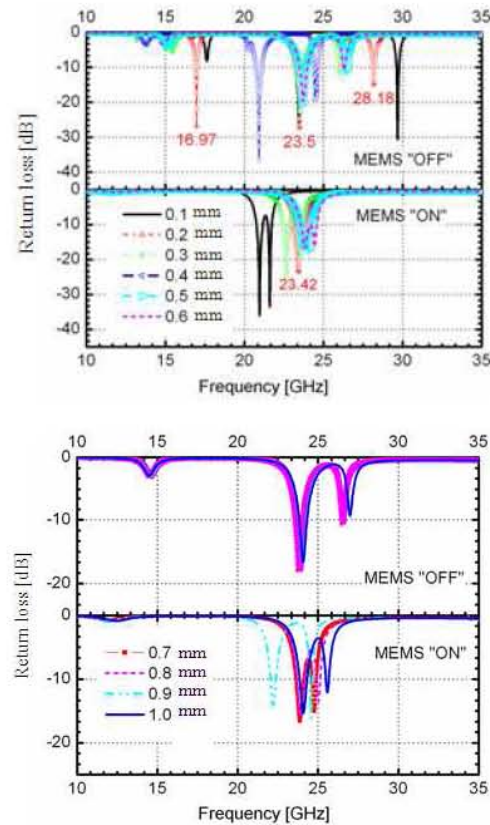


Fig. 2: Return loss for different MEMS contact width for “OFF” and “ON” states

width of MEMS switch is chosen at 0.2 mm for optimum performance of the antenna as mentioned earlier. It is also mentioned that the centre resonant frequency when the MEMS contacts are in the “OFF” states does not deviate appreciably from the resonant frequency when the MEMS contacts are in the “ON” states.

Effects of wing patch width: The simulation has done for varying the wing patch width by maintaining the length L_w of the wing at 5 mm and considering Alumina as a MEMS bridge material. The length is varied from 1-4 mm in 1 mm step and the results are presented in Fig. 4. The Fig. 4 shows that the antenna loses its performance when the wing patch width is 4 mm, the same width as the centre patch width. It also shows that return losses decrease with the increase in width of the wing patch. The multi-band antenna can be obtained by reducing the width of the wing patches. It is observed that there are three resonant frequencies, namely 16.97, 23.5 and 28.18 GHz with the return losses of 26.86, -27.4 and -14.9 dB, respectively for a wing width of 2 mm, when the MEMS are in the “OFF” states.

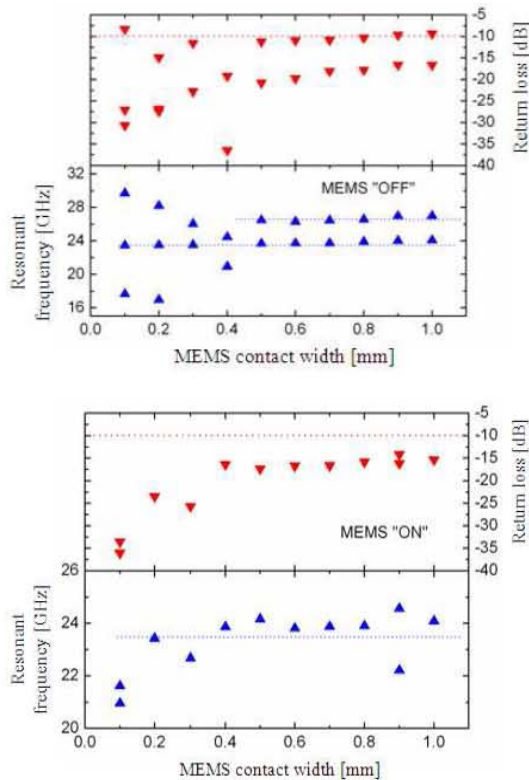


Fig. 3: Return loss and resonant frequency for different MEMS contact width for “OFF” and “ON” states

The single resonant frequency of 23.42 GHz with return loss of -23.47 dB has been observed for the same wing dimensions when the MEMS are in the “ON” states. It is said that the antenna behaves like a single patch antenna when the MEMS are in the “ON” states.

Effects of MEMS bridge materials: The simulation is done by choosing Alumina, GaAs, SiN and Teflon as a MEMS cantilever materials by varying the wing patch width maintaining the MEMS contact width at 0.1 mm. The simulation results of Fig. 3 show that wider the MEMS contact width, larger the values of return losses for Alumina as MEMS cantilever bridge. These phenomena are also applicable to other MEMS bridge materials with wing widths of 3 and 4 mm as shown in Fig. 5.

The effects of MEMS cantilever bridge material on the antenna return losses are shown in Fig. 6 for four different MEMS bridge materials when the MEMS contacts are in the “OFF” and “ON” states, by maintaining optimized wing width. The resonant frequencies and the return losses for different materials are presented in Table 2.

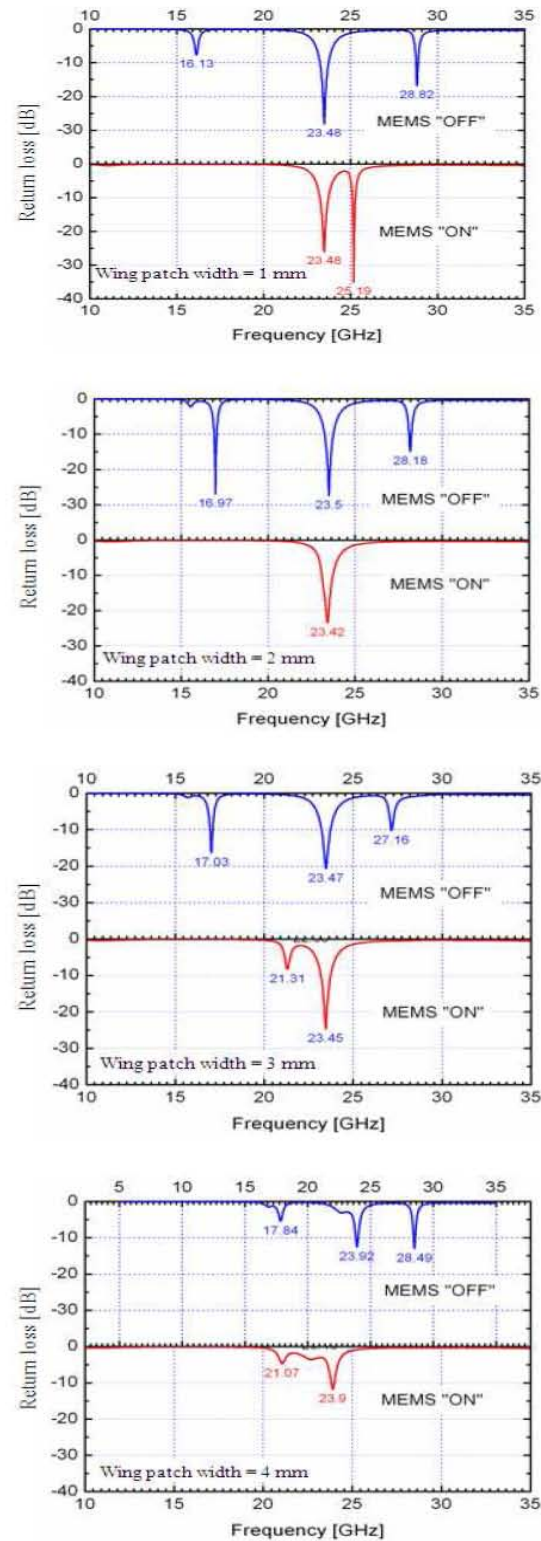


Fig. 4: Return losses for four antennas with different wing patch width

Table 2: Resonant frequencies and return losses for different MEMS cantilever material

MEMS material	OFF state resonant frequency and return loss			ON state resonant frequency and return loss	
	f_{1F} , S_{11} (dB)	f_{2F} , S_{11} (dB)	f_{3F} , S_{11} (dB)	f_{1N} , S_{11} (dB)	f_{2N} , S_{11} (dB)
Alumina (9.4)	16.97, -26.86	23.50, -27.4	28.18, -14.9	23.42, 23.47	-
GaAs (12.9)	16.41, -12.24	23.42, -25.45	27.11, -11.91	23.36, -20.06	-
SiN (9)	16.76, -29.56	23.56, -26.31	27.70, -13.69	20.90, -38.69	21.91, -25.72
Teflon (2.1)	21.46, -31.74	24.28, -19.99	-	20.90, -38.69	21.91, 25.72

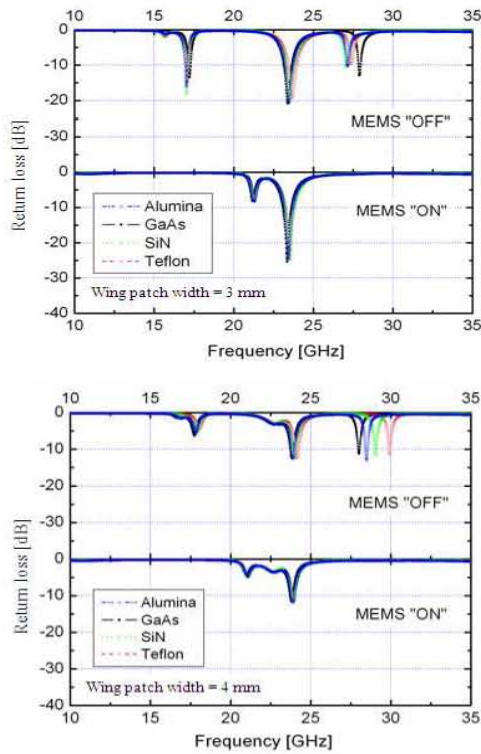


Fig. 5: Return losses for four antennas with different wing patch width for various MEMS cantilever bridge material

It is observed that there are three resonant frequencies for Alumina, GaAs and SiN materials when the MEMS are in the “OFF” states whereas Teflon provides two resonant frequencies. When the MEMS contacts are in the “ON” states, Alumina and GaAs provide single resonant frequency, whereas SiN and Teflon materials provide two resonant frequencies. It is also observed that in “ON” states of MEMS contact has no effect of shifting the resonant frequencies when the materials are either SiN or Teflon. Therefore, multi-band antenna can be made by choosing Alumina as MEMS cantilever bridge material for operating three different frequencies (16.97, 23.5/23.42 and 28.18 GHz). By choosing SiN as MEMS cantilever bridge material, it has been observed that the antenna is able to operate at different frequencies (16.97, 20.9, 21.91, 23.56 and 27.7 GHz).

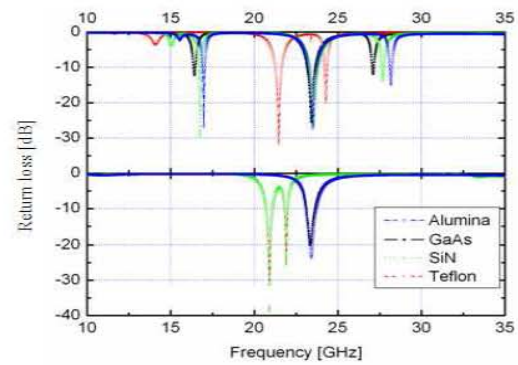


Fig. 6: Return losses for four antennas with different MEMS cantilever bridge material

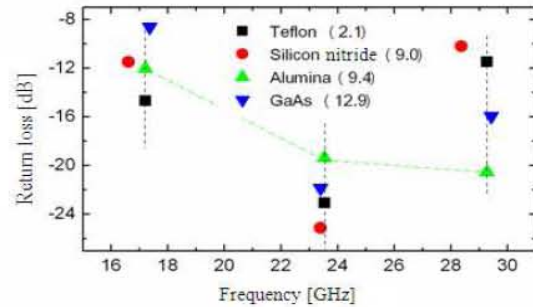


Fig. 7: Return loss of the antenna for different types of MEMS bridge materials when the switches are at “OFF” states

The simulation has done by increasing the distance between patch and MEMS contact from 5-10 μm . The return loss versus the resonant frequency with different MEMS bridge materials is shown in Fig. 7 when the MEMS contacts are in the “OFF” states. It is observed that there are three resonant frequencies for all the materials. The lower, centre and higher resonant frequencies occur almost at the same frequency irrespective of the materials used.

The return losses and the resonant frequencies of the antenna for different types of MEMS bridge materials are shown in Fig. 8. Here the MEMS contacts are in the “ON” states for 10 μm gap between contacts and patches, which shows that there is only single resonant frequency irrespective of the MEMS bridge materials,

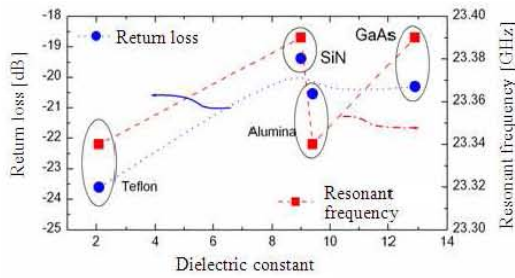


Fig. 8: Return loss of the antenna for different types of MEMS bridge materials when the switches are at “ON” states

this is differ from SiN and Teflon materials for a separation of 5 μm . It is mentioned that larger separation between MEMS switches and patches need higher turn-on voltage to contact patches.

Therefore, it can be concluded that Alumina, as the MEMS cantilever bridge materials, provides optimum antenna performance for operating at three different frequency bands. However, there is no need of MEMS switch for Alumina materials since there is no appreciable shift of resonant frequency when the MEMS contacts are in the “ON” states or in the “OFF” states for one particular frequency band. However, SiN as MEMS cantilever bridge material provides five resonant frequencies, three in the “OFF” states and two in the “ON” states.

The radiation pattern of the resonant frequencies is shown in Fig. 9 for Alumina when the MEMS contacts are in the “OFF” and “ON” states for 5 μm separation.

DISCUSSIONS

The variation of resonant frequency for different type of MEMS bridge materials may be due to formation of parasitic capacitances and these capacitances value changes with the variation of dielectric constant. The dielectric constant $\epsilon = \epsilon' + j\epsilon''$ is also a function of frequency and the variation is very complex at very high frequency.

It is thought that the centre frequency is generated by the centre patch whereas the adjacent frequencies are generated in the presence of two side wing patches which may result parasitic capacitances connected to centre and the wing patches. There is no radiation from the back side of the antenna which is due to the presence of the ground plan.

Reconfigurable antenna can be made by using SiN as MEMS cantilever bridge materials to operate in five operating frequencies whereas Teflon material can also be used for reconfigurable antenna to operate at four different frequencies.

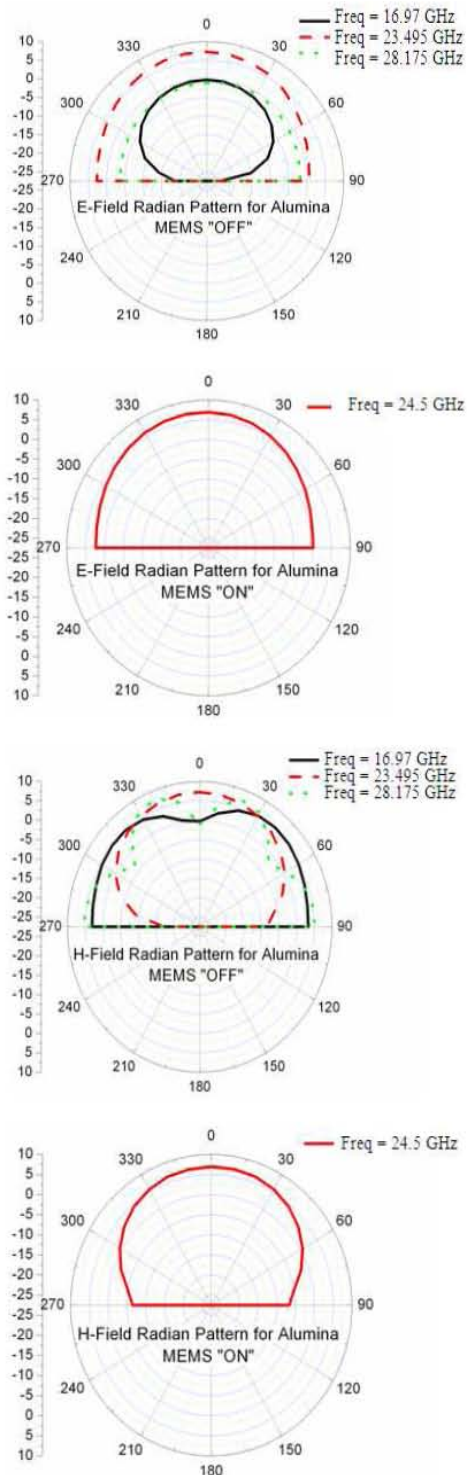


Fig. 9: Radiation pattern for the total gain at E- and H-planes for different resonant frequencies when the MEMS contacts are in “OFF” and “ON” states for Alumina as MEMS materials

CONCLUSION

Multi-band antenna has been designed by placing and optimizing the dimension of two adjacent patches. Additional resonant frequencies have been obtained by incorporating MEMS switches. It is concluded that the MEMS cantilever beam material plays an important role for providing antenna to operate at multi-band frequencies. A triple-band antenna operating at 16.97, 23.5 and 28.18 GHz is possible by selecting Alumina as MEMS bridge material. A penta-band reconfigurable antenna is possible by constructing MEMS bridge using SiN material. The antenna can be operated at 16.76, 23.56 and 27.7 GHz when the MEMS switches are in the "OFF" states and can be operated at 20.9 and 21.91 GHz when the MEMS switches are in the "ON" states. The proposed reconfigurable antenna can be implemented with easy fabrication process steps by the Sandwich method of fabrication. This study has shown the possibility of using the antenna for multi-band communication applications.

ACKNOWLEDGMENT

This study is funded by the Fundamental Research Grant Scheme by Ministry of Higher Education Malaysia through the Research Centre, International Islamic University Malaysia, Grant No. IIUM/504/RES/G/14/3/05/FRGS 0106-28.

REFERENCES

1. Tomiyasu, K., 2003. Conceptual reconfigurable antenna for 35 GHz high-resolution spaceborne synthetic aperture radar. *IEEE. Trans. Aerospace Elect. Syst.*, 39: 1069-1074. DOI: 10.1109/TAES.2003.1238758
2. Aberle, J.T., S.H. Oh, D.T. Auckland and S.D. Rogers, 2003. Reconfigurable antennas for wireless devices. *IEEE. Antennas Propagat. Mag.*, 45: 148-154. DOI: 10.1109/MAP.2003.1282191
3. Huff, G.H., J. Feng, S. Zhang, G. Cung and J.T. Bernhard, 2004. Directional reconfigurable antennas on laptop computers: Simulation, measurement and evaluation of candidate integration positions. *IEEE. Trans. Antennas Propagat.*, 52: 3220-3227. DOI: 10.1109/TAP.2004.836425
4. Weedon, W.H., W.J. Payne and G.M. Rebeiz, 2001. MEMS-switched reconfigurable antennas. *Proceeding of the IEEE Antennas Propagation Society International Symposium*, July 8-13, IEEE Xplore Press, Boston, MA, USA., pp: 654-657. DOI: 10.1109/APS.2001.960181
5. Peroulis, D., K. Sarabandi and L.P.B. Katehi, 2005. Design of reconfigurable slot antennas. *IEEE. Trans. Antennas Propagat.*, 53: 645-654. DOI: 10.1109/TAP.2004.841339
6. Tong, C.E. and R. Blundel, 1994. An annular slot antenna on a dielectric half-space. *IEEE. Trans. Antennas Propagat.*, 42: 967-974. DOI: 10.1109/8.299599
7. Yao, J.J. and M.F. Chang, 1995. A surface micromachined miniature switch for telecommunications applications with signal frequencies from DC up to 4 GHz. *Proceeding of the 8th International Conference on Solid-State Sensors and Actuators and Eurosensors Transducers*, June 25-29, IEEE Xplore Press, USA., pp: 384-387. http://ieeexplore.ieee.org/xpl/freeabs_all.jsp?arnumber=721827
8. Suryanarayana, P., A.A. Naik, C.H. Sridhar and V.S. Murthy *et al.*, 2007. Process development of GaAs based RF MEMS. *Proceeding of the International Workshop on Physics of Semiconductor Devices*, Dec. 16-20, IEEE Xplore Press, Mumbai, pp: 699-701. DOI: 10.1109/IWPSD.2007.4472616
9. Hah, D., E. Yoon and S. Hong, 2000. A low-voltage actuated micromachined microwave switch using torsion springs and leverage. *IEEE. Trans. Microwave Theor. Tech.*, 48: 2540-2545. DOI: 10.1109/22.899010
10. Park, J.Y., G.H. Kim, K.W. Chung and J.U. Bu, 2001. Monolithically integrated micromachined RF MEMS capacitive switches. *Sensors Actuat. A Phys.*, 89: 88-94. DOI: 10.1016/S0924-4247(00)00549-5
11. Pacheco, S.P., L.P.B. Katehi and C.T.C. Nguyen, 2000. Design of low actuation voltage RF MEMS switch. *Proceeding of the MTT-S International Microwave Symposium*, June 11-16, IEEE Xplore Press, Boston, MA, USA., pp: 165-168. DOI: 10.1109/MWSYM.2000.860921
12. Cetiner, B.A., H. Jafarkhani, J.Y. Qian, H.J. Yoo, A. Grau and F. DeFlaviis, 2004. Multifunctional reconfigurable MEMS integrated antennas for adaptive MIMO systems. *IEEE. Commun. Mag.*, 42: 62-70. DOI: 10.1109/MCOM.2004.1367557
13. Huff, G.H. and J.T. Bernhard, 2006. Integration of Packaged RF MEMS switches with radiation pattern reconfigurable square spiral microstrip antennas. *IEEE. Trans. Antennas Propagat.*, 54: 464-469. DOI: 10.1109/TAP.2005.863409

14. Haridas N., A.T. Erdogan, T. Arslan, A. J. Walton and S. Smith *et al.*, 2008. Reconfigurable MEMS antennas. Proceeding of the NASA/ESA Conference on Adaptive Hardware and Systems, June 22-25, IEEE Xplore Press, Noordwijk, pp: 147-154. DOI: 10.1109/AHS.2008.28
15. Piazza, D., N.J. Kirsch, A. Forenza, R.W.J. Heath and K.R. Dandekar, 2008. Design and evaluation of a reconfigurable antenna array for MIMO systems. IEEE. Trans. Antennas Propagat., 56: 869-881. DOI: 10.1109/TAP.2008.916908
16. Grag, R., P. Bhartia, I. Bahl and A. Ittipiboon, 2001. Microstrip Antenna Design Handbook. Artech House, ISBN: 0890065136, pp: 845.